RSC Advances

ROYAL SOCIETY OF CHEMISTRY

www.rsc.org/advances

RSC Advances

ARTICLE

Soy protein isolate based films cross-linked by epoxidized soybean oil

Received 00th January 20xx,
Accepted 00th January 20xx

DOI: 10.1039/x0xx00000x

www.rsc.org/

Changlei Xia,[b] La Wang,[a] Youming Dong,[a] Shifeng Zhang,[a,*] Sheldon Q. Shi,[b,*] Liping Cai [b] and Jianzhang Li [a,*]

Epoxidized soybean oil (ESO) is an environmental-friendly cross-linking agent derived from soybean, owning multiple epoxy groups in a molecular. It could effectively improve tensile strength and water resistance of soy protein isolate (SPI) based films. The properties of the SPI-based films was characterized by the X-ray diffraction and attenuated total reflectance Fourier transform infrared spectroscopy. The best performance of the SPI-based film was achieved when the ESO addition was 2.5%, whose tensile modulus, tensile strength and 10% offset yield strength were increased to 265.0 MPa, 9.8 MPa and 6.8 MPa, respectively. Compared to the un-treated SPI-based films, they were counted the increases of 695.6%, 139.8%, and 246.6%, respectively. However, its elongation at break was decreased by 67.6% due to the cross-linking between SPI and ESO. The SPI-based film modified by 5% ESO had the best water-resistant property and reduced the 24-hour water absorption from 209.1% to 45.9%, which was a significant decrease of 78.1%.

Introduction

Driven by the environmental concerns caused by using petrochemical based synthetic polymers,[1,2] interest has arisen in using renewable, degradable, and compostable films and coatings from polysaccharide, protein and lipid biopolymers for packaging, mulching and other industrial applications.[3–5] As a by-product in the edible oil industry, soy protein isolate (SPI) has advantages of inexpensive, biocompatible, renewable, etc., providing an environmentally-conscious alternative to fossil fuel source.[6–9] However, the drawbacks, such as low strength and poor water resistance,[10,11] limit the applications of SPI-based products.

Many efforts have been made to enhance the performances of SPI-based films, such as improving the processing methods,[12–14] blending or compositing with natural materials,[15] treated by enzyme,[16] cross-linked by chemicals,[6,17–21] etc. Among them, chemical cross-linking of the proteins is proved to be one of the most promising ways for enhancing the properties of the films. The most common used crosslinking agents were aldehydes, such as formaldehyde, glutaraldehyde and glyoxal,[19,22–24] phenolic compounds,[18,25] and epoxy compounds.[6,26] However, the use of these compounds to fabricate food packaging is not particularly safe considering their cytotoxicity. To address this concern, some of the biomass-based cross-linking agents, such as genipin[20] and dialdehyde starch,[21] were developed. However, the properties of the cross-linked films, especially the tensile strength, are still expected to be improved.

To improve the tensile strength and water-resistant properties of SPI-based films without introducing very toxic chemicals, epoxidized soybean oil (ESO) was employed as a cross-linking agent in this research. As one of the important vegetable oil-based polymers, ESO is synthesized by the epoxidation of the double bonds of soybean oil.[27] Compared with petroleum-based polymers, ESO is a preferred bio-material owing to the advantages of bio-renewable, biocompatible, and biodegradable.[28] The multiple epoxy groups of the ESO molecule are able to cross-link with SPI molecule owing to their abundant of amino groups, which is able to form a network structure between SPI and ESO to enhance the tensile strength and water-resistant properties of SPI-based films.

The objective of this study was to fabricate the cross-linked SPI-based films using the centrifugal casting method. The effects of ESO on the mechanical properties and water resistance behavior of the SPI-based films were investigated.

Experimental

Materials

The SPI with a protein content of over 90% was from Sausage Maker, Inc., USA. Vikoflex® 7170 ESO with the oxirane values more than 6.80%, was supplied by Arkema Chemicals Company, USA. The 3-Glycidoxypropyl-trimethoxysilane (GPTMS) with a purity of 97% and the biotechnology grade glycerol were supplied by Acros Organics and bioWORLD, USA, respectively. The sodium hydroxide (NaOH) solution (10%,

[a] MOE Key Laboratory of Wooden Material Science and Application, Beijing Key Laboratory of Wood Science and Engineering, MOE Engineering Research Center of Forestry Biomass Materials and Bioenergy, Beijing Forestry University, Beijing 100083, China. E-mails: zhangshifeng2013@126.com; lijianzhang126@126.com.
[b] Department of Mechanical and Energy Engineering, University of North Texas, Denton, TX 76203, USA. E-mail: Sheldon.Shi@unt.edu.

Table 1 Feedstocks for preparing the SPI-based films.

Film	SPI [a] (g)	DI water [b] (mL)	NaOH [c] (g)	ESO [e] (g)	ESO [e] (%) [d]	GPTMS [f] (g)	GPTMS [f] (%) [d]
SPI	4	40	0.5	-	-	-	-
SPI/GPTMS	4	40	0.5	-	-	0.4	10
SPI/GPTMS/ESO-1%	4	40	0.5	0.04	1	0.4	10
SPI/GPTMS/ESO-2.5%	4	40	0.5	0.1	2.5	0.4	10
SPI/GPTMS/ESO-5%	4	40	0.5	0.2	5	0.4	10
SPI/GPTMS/ESO-10%	4	40	0.5	0.4	10	0.4	10
SPI/GPTMS/ESO-15%	4	40	0.5	0.6	15	0.4	10
SPI/ESO-2.5%	4	40	0.5	0.1	2.5	-	-

[a] SPI = soy protein isolate; [b] DI water = deionized water; [c] 10% NaOH aqueous solution; [d] the percentages were calculated based on the amount of SPI (4 g); [e] ESO = epoxidized soybean oil; [f] GPTMS = 3-Glycidoxypropyl-trimethoxysilane.

w/v) was prepared using NaOH beads (≥97%, Acros Organics) and deionized (DI) water that was from the Millipore Milli-Q Integral Water Purification System.

Preparation of the SPI-based films

Using the method of centrifugal casting, a spin caster (AMT-SC5052, Affine Materials Technology, USA) with a motor (BQB 56C34D2096F P, Marathon, USA) of 3450 RPM was employed to fabricate the films. The centrifugal casting method is able to accelerate the evaporation of water from the mixture. The experiments were performed in a fume hood with a relative humidity of about 50% and a temperature of 20 °C. A three-step process was carried out:

1) The SPI films were successively made by mixing 4 g SPI with 40 mL DI water, 2 g glycerol and 0.5 g 10% NaOH solution. Different contents of ESO and/or GPTMS were added for different types of films as shown in Table 1. All the mixtures were magnetically stirred for 1 h before the next process.
2) The mixtures were pulled into the spin caster and then centrifuged for 4 h. The films were formed on the surface of cylindrical container with 5 cm in height and 12.7 cm in diameter.
3) The films were thermal treated at 105 ± 3 °C for 4 h and stored in a conditioning room with a relative humidity of 50 ± 2% and a temperature of 20 ± 3 °C.

ATR FT-IR analysis

The attenuated total reflectance (ATR) Fourier transform infrared spectroscopy (FT-IR) was used to examine the chemical structures of the films. A Nicolet 6700 FT-IR spectrometer (Thermo Scientific, USA) with an ATR accessory was employed. The wavelength range was between 650 to 4000 cm^{-1}.

XRD analysis

The X-ray diffraction (XRD) analysis was carried out with an XRD-6000 meter (Shimadzu, Japan, Cu Kα radiation, λ = 1.54060Å), operating at 40 kV and 40 mA. The samples were scanned in the continuous scanning mode with the 2θ from 10° to 60° (2θ) at a rate of 2°/min, where θ was the incident angle of the X-ray beam on the sample. The relative crystallinity index (RCI) was calculated directly by the XRD instrument with the equation:

$$\mathrm{RCI}\ (\%) = A_c \times (A_c + A_a)^{-1} \times 100 \qquad (1)$$

where A_c is the area of the crystalline region and A_a is the area of the amorphous region. Three replicates were carried out for each composition.

Mechanical property tests

The tensile tests of the specimens were carried out at a room temperature in accordance with the procedures described in ASTM D882 standard using the Shimadzu AGS-X tester with a 76.2 mm (3 inch) gauge length. Twelve replicates were used for each film. The specimen dimensions were 18 × 120 mm and the cross section of the narrow section was 76.2 × 12.7 mm (length × width). A crosshead speed of 50 mm min^{-1} was used.

SEM observation

A Quanta 200 environmental scanning electron microscope (SEM) with an accelerating voltage of 15 kV and a magnification of 2,000× was used to observe the tensile fracture failure mode of the specimens. Prior to the observation, the specimens were sputter-coated with gold for 5 minutes to avoid charging under the electron beam.

Water absorption tests

Six specimens of each film with a dimension of 20 × 20 mm were used for the moisture content measurements and water absorption tests. Twenty four-hour water submersion tests were carried out in accordance with the ASTM D1037 standard for the determination of the water absorption. In addition, the moisture contents after equilibrium in the conditioning chamber at a relative humidity of 50 ± 2% and a temperature

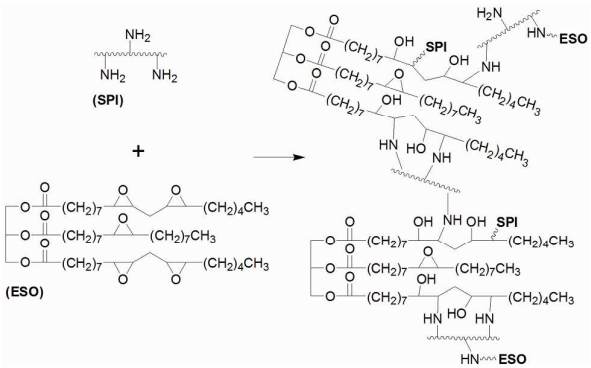

Fig. 1 Cross-linking reaction mechanism of SPI and ESO.

of 20 ± 3 °C for 10 days and water submersion for 24 h were determined in according with the ASTM D4442 standard.

Results and discussion

Characterization of the SPI-based films

SPI contains more than 90% proteins, counting 7.7% arginine (Arg), 6.8% lysine (Lys), and 2.5% cysteine (Cys) that has abundant of $–NH_2$ groups.[29] The total percentage of that type of amino acids can be 17.0% in the protein. ESO contains multiple epoxy groups per molecular.[12,27,30] The $–NH_2$ groups and the epoxy groups can react with each other through the ring opening polymerization.[6,31] The cross-linking reactions are showed in Fig. 1. The multiple $–NH_2$ groups on the SPI and multiple epoxy groups on the ESO were able to cross-link the two feedstocks, resulting in a cross-linked film.

The images of the films are displayed in Fig. 2. SPI, SPI/GPTMS, SPI/GPTMS/ESO-1%, and SPI/GPTMS/ESO-2.5% films showed very good transparency. With the increase in ESO amount, the films (SPI/GPTMS/ESO-5%, SPI/GPTMS/ESO-10%, and SPI/GPTMS/ESO-15% films) became less transparent. Compared to the good transparency and uniform distribution of the SPI/GPTMS/ESO-2.5% film, the SPI/ESO-2.5% film without GPTMS was close to opaque and very heterogeneous, suggesting a poor distribution of ESO in SPI matrix. To improve the compatibility between SPI and ESO, a silane coupling agent, GPTMS, was employed to disperse the hydrophobic ESO into hydrophilic SPI.[32–34] Compared to the images of SPI/GPTMS/ESO-2.5% and SPI/ESO-2.5% films (Fig 2), it is easily seen the effect of GPTMS on the compatibility of the films, reflecting as relatively clear and transparent of the SPI/GPTMS/ESO-2.5% film.

Fig. 2 Images of the SPI-based films.

The ATR FT-IR spectra of the SPI powder and SPI-based films are presented in Fig. 3. The broad absorption band observed around 3275 cm^{-1} is attributable to free and bounded O–H and N–H groups. The increase in intensity at 3275 cm^{-1} was observed after the SPI being fabricated into the films, due to the abundant –OH group was introduced into the system. The characteristic C–H stretching of CH_2 and CH_3 groups of saturated structures was observed in 2925 and 2855 cm^{-1}, and C–H bending band was showed in 1455 cm^{-1}. The peak at 1743 cm^{-1} was corresponding to the stretch of C=O groups in COOH or COOR. The spectra of the SPI film showed relevant peaks at

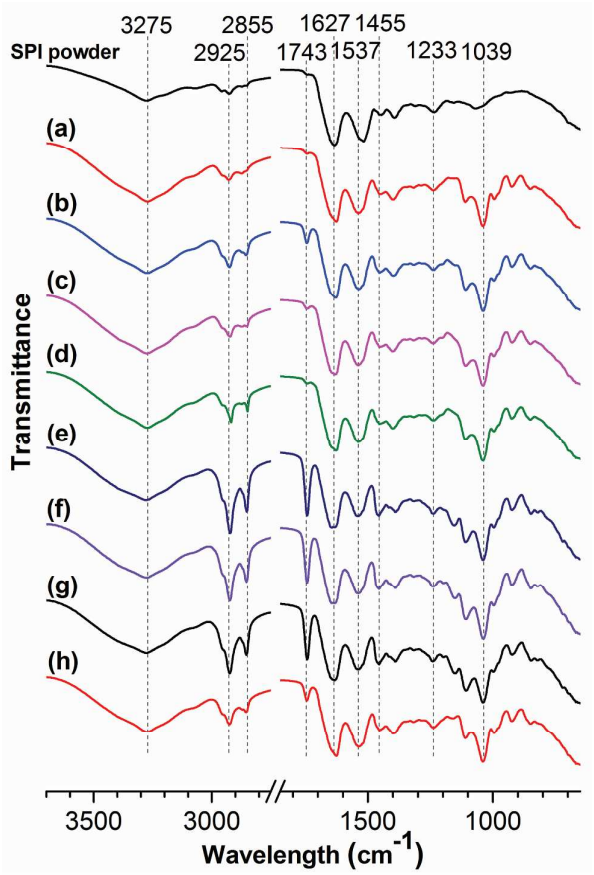

Fig. 3 ATR FT-IR spectra of SPI powder, and films of SPI (a), SPI/GPTMS (b), SPI/GPTMS/ESO-1% (c), SPI/GPTMS/ESO-2.5% (d), SPI/GPTMS/ESO-5% (e), SPI/GPTMS/ESO-10% (f), SPI/GPTMS/ESO-15% (g) and SPI/ESO-2.5% (h).

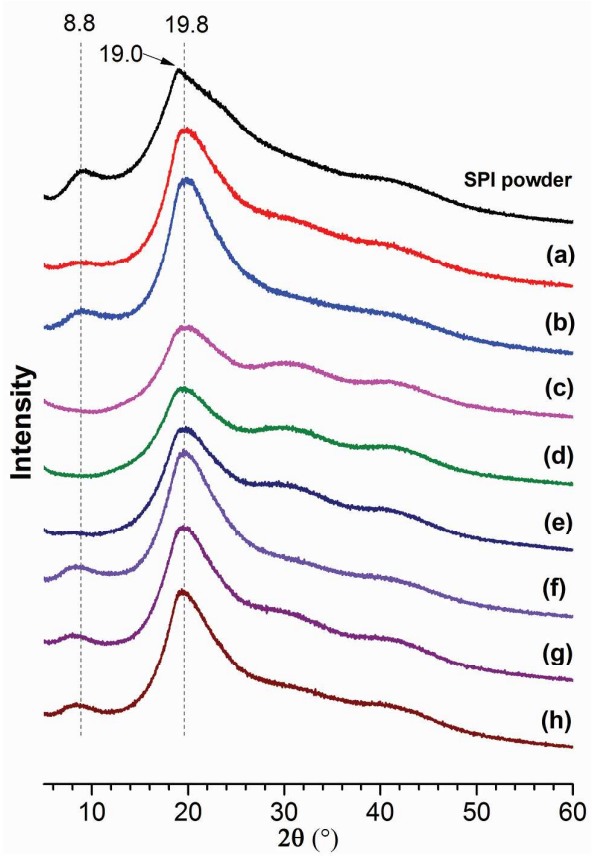

Fig. 4 XRD patterns of SPI powder, and films of SPI (a), SPI/GPTMS (b), SPI/GPTMS/ESO-1% (c), SPI/GPTMS/ESO-2.5% (d), SPI/GPTMS/ESO-5% (e), SPI/GPTMS/ESO-10% (f), SPI/GPTMS/ESO-15% (g) and SPI/ESO-2.5% (h).

1627, 1537 and 1233 cm^{-1} (Fig. 3), which were characteristic of amide I (C=O stretching), amide II (N–H bending), and amide III (C–N and N–H stretching), respectively. The result was consistent with the findings in the literature.[35] The peak at 1039 cm^{-1} belongs to C–O stretching. Compared to the SPI powder, the FT-IR peaks of the SPI film at 3275 and 1039 cm^{-1} were increased, owing to the glycerol in the SPI film. The intensity of the peak at 1743 cm^{-1} (C=O groups in COOH or COOR) became stronger after adding the GPTMS ((a) to (b) in Fig. 3), due to the amphiphilic property of GPTMS. The same phenomenon was found when the sodium dodecyl sulfate (SDS) was employed.[36] The intensities at 1743 cm^{-1} were decreased after adding 1% and 2.5% ESO ((b) to (c) and (d) in Fig. 3), while increased at the films contain 5%, 10%, and 15% ESO. There could be two reasons: 1) the reactions between ESO and SPI reduced the density of C=O groups (in COOH or COOR) on the surface of the film; 2) the increased amounts of ESO introduced abundant C=O groups (in COOR) existing on the surface. Compared to the FT-IR spectra of the SPI/GPTMS/ESO-2.5% film ((d) in Fig. 3) with the SPI/ESO-2.5% film ((h) in Fig. 3), without GPTMS in the SPI/ESO-2.5% film, ESO located on the surface of the film with poor distribution and presented a relatively strong intensity at 1743 cm^{-1}, indicating that GPTMS can help dispersing hydrophobic ESO into hydrophilic SPI in according with the peak intensity at 1743 cm^{-1} of the SPI/GPTMS/ESO-2.5% film.

Table 2 Crystallinity of the SPI powder and SPI-based films.

Sample	RCI [a] (%)
SPI powder	30.1 (0.7) [b]
SPI	29.5 (0.9)
SPI/GPTMS	34.0 (0.4)
SPI/GPTMS/ESO-1%	23.5 (0.9)
SPI/GPTMS/ESO-2.5%	22.9 (1.0)
SPI/GPTMS/ESO-5%	28.0 (1.0)
SPI/GPTMS/ESO-10%	36.4 (0.4)
SPI/GPTMS/ESO-15%	34.1 (1.0)
SPI/ESO-2.5%	33.7 (0.4)

[a] RCI = Relative crystallinity index; [b] mean (standard deviation).

XRD patterns of SPI powder and the SPI-based films are presented in Fig. 4. Peaks at 2θ ≈ 8.8° and 19.8° represented the α-helix and β-sheet structures of SPI secondary structure, respectively.[6, 37] The β-sheet XRD peaks of SPI-based film were slightly greater than the SPI powder (19.0°), because of the effect of the small molecular (glycerol) in the SPI-based films, which was able to reduce the lattice constant. The RCIs were calculated in according with Eq. (1), and the results are shown in Table 2. The lowest RCI was found in the SPI/GPTMS/ESO-2.5% film (RCI = 22.9%), which was reduced by 22.4% compared with the SPI film (RCI = 29.5%). The results of ANOVA tests showed that the decrease was significant at the probability level of $\alpha = 0.01$ (P-value = 0.0022). The crystallinity of SPI/GPTMS/ESO-2.5% film decreased significantly, since the molecular chains could not move smoothly after the formation of the crosslinking networks.[6]

Mechanical properties

The results of tensile tests (tensile modulus (TE), tensile strength (TS), 10% offset yield strength (YS), and elongation at break) are summarized in Table 3 and the average engineering strain-stress curves of the films are shown in Fig. 5. Generally, it was found that the TE, TS and YS of SPI-based films tended to increase with the added ESO amount to reach a maximum at 2.5% ESO, and then decreased with the further increase in ESO. Obviously, the SPI/GPTMS/ESO-2.5% film had the greatest TE (265.0 MPa), TS (9.8 MPa) and YS (6.8 MPa), which were counted the increases of 695.6%, 139.8%, and 246.6%, respectively, compared with those mechanical properties of the SPI film (TE = 33.3MPa, TS = 4.1 MPa, and YS = 2.0 MPa). TE, TS and YS were analysed by ANOVA tests and the results showed the increases were significant at the probability level of $\alpha = 0.001$, in which the P-values were 2.4×10^{-5}, 1.6×10^{-4}, and 3.4×10^{-6}, respectively. However, the elongation at break was reduced by 67.6%, owing to the formation of the cross-linking network between SPI and ESO (Fig. 1).[6] The results

Table 3 Mechanical properties (tensile modulus, tensile strength, 10% offset yield strength, and elongation at break) and thicknesses of the SPI-based films.

Film	Thickness (mm)	Tensile modulus (MPa)	Tensile strength (MPa)	10% offset yield strength (MPa)	Elongation at break (%)
SPI	0.261 (0.012) [a]	33.3 (2.6)	4.1 (0.2)	2.0 (0.1)	213.5 (12.4)
SPI/GPTMS	0.241 (0.009)	78.3 (6.9)	5.7 (0.6)	3.5 (0.1)	65.7 (13.9)
SPI/GPTMS/ESO-1%	0.239 (0.019)	96.6 (6.0)	7.0 (0.3)	4.0 (0.2)	75.1 (3.7)
SPI/GPTMS/ESO-2.5%	0.261 (0.013)	265.0 (14.5)	9.8 (0.6)	6.8 (0.2)	69.1 (10.9)
SPI/GPTMS/ESO-5%	0.259 (0.022)	132.1 (13.7)	8.9 (0.2)	4.8 (0.1)	83.1 (3.6)
SPI/GPTMS/ESO-10%	0.264 (0.004)	177.8 (20.0)	7.6 (0.3)	5.2 (0.1)	64.8 (7.2)
SPI/GPTMS/ESO-15%	0.328 (0.008)	62.0 (4.8)	4.8 (0.3)	3.1 (0.1)	61.0 (7.0)
SPI/ESO-2.5%	0.342 (0.015)	79.8 (6.5)	3.7 (0.2)	2.8 (0.1)	97.7 (19.4)

[a] mean (standard deviation).

indicated that ESO could significantly enhance the TE, TS, and YS of SPI-based film, but reduce the elongation at break. The TE, TS, and YS of the SPI/GPTMS/ESO-2.5% film were increased by 231.9%, 163.6%, and 142.2%, respectively, comparing with those of the SPI/ESO-2.5% film. It was suggested that the compatibility between the SPI and ESO was improved by the addition of GPTMS, because GPTMS help dispersing the hydrophobic ESO into the hydrophilic SPI, which was consistent with the images in Fig. 2.

The tensile strength of the SPI-based films with different cross-linking agents were compared and are presented in Table 4. The SPI-based films cross-linked by ESO had the highest TS of 9.8 MPa with an increase of 139.8% among the biomass-based agents including genipin (4.6 MPa with a 42.9% increase)[20] and dialdehyde starch (7.84 MPa with a 23.7% increase).[21] Compared to the SPI-based films cross-linked by other chemicals, including 1,2,3-propanetrioldiglycidyl-ether (PTGE) (TS = 6.21 MPa with a 197.1% increase),[6] ferulic acid (TS = 2.602 MPa with a 62.8% increase),[17] and formaldehyde (TS = 1.69 MPa with a 164.1% increase),[19] the TS of SPI-based film fabricated in this work was still larger then others (Table 4), though the increase might not be the largest. Based on the detailed literature review, the best cross-linking agent was the resorcinol,[18] and the TS (24.7 MPa with a 404.1% increase) of treated SPI-based film was higher than that in this work. However, resorcinol is a cytotoxic chemical which may cause some environmental concerns. In general, by taking the film performance and environmental issues into account, the SPI-based film cross-linked by ESO is a unique technology because it improves the tensile strength without compromising the environmental sustainability.

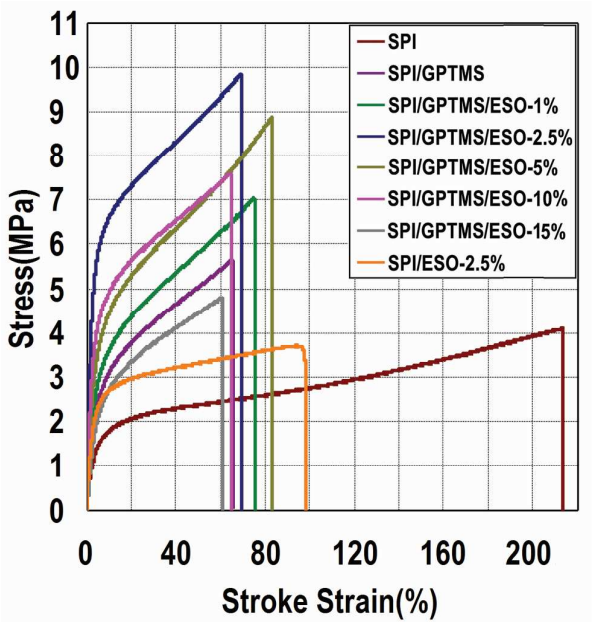

Fig. 5 Stress-strain curves of SPI-based films.

Table 4 Comparison of tensile strengths of SPI-based films cross-linked by various agents.

Cross-linking agent	TS of films (MPa) [c]		Increase (%) [d]	Reference
	Control	Treated		
ESO [a]	4.1	9.8	139.8	this work
PTGE [b]	2.09	6.21	197.1	Xu[6]
Ferulic acid	1.598	2.602	62.8	Ou[17]
Resorcinol	4.9	24.7	404.1	Reddy[18]
Formaldehyde	0.64	1.69	164.1	Chen[19]
Genipin	3.22	4.6	42.9	Gonzalez[20]
Dialdehyde starch	6.34	7.84	23.7	Rhim[21]

[a] ESO = epoxidized soybean oil; [b] PTGE = 1,2,3-propanetrioldiglycidyl-ether; [c] TS = tensile strength; [d] Increase was calculated from the TS of control and treated samples from relative literature.

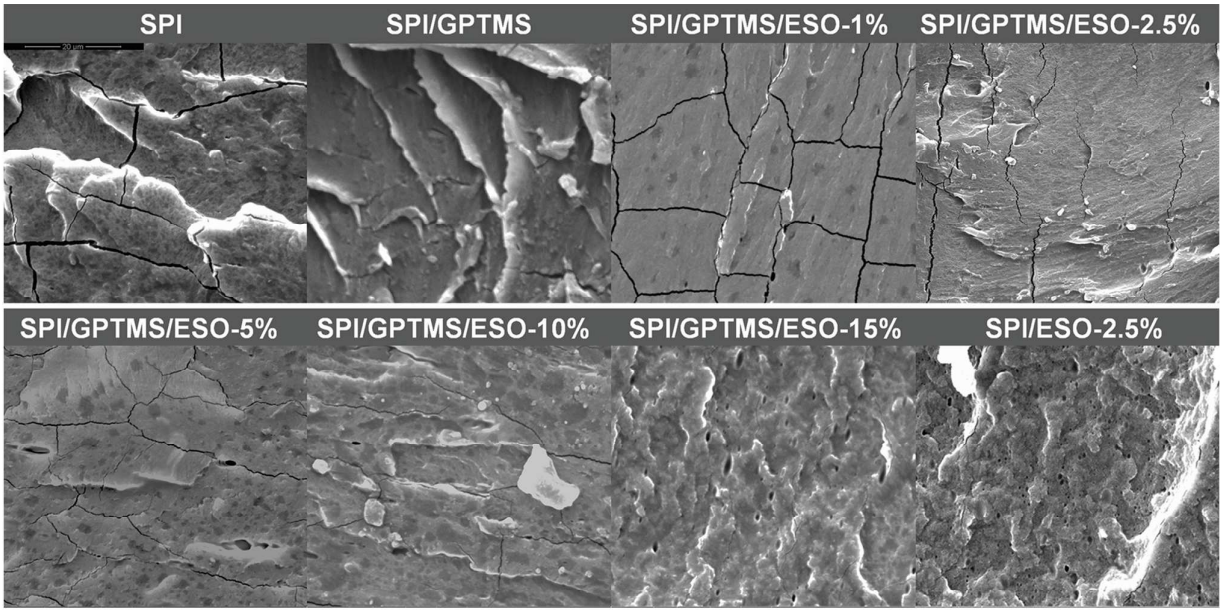

Fig. 6 SEM images of cross-sections of the SPI-based films.

Micromorphology

The cross-sectional morphology of tensile fracture surfaces are presented in Fig. 6. The defects and inhomogeneous characteristics were obvious in the SPI film. After GPTMS was introduced, the surface was not improved. The relatively homogeneous surfaces were also observed in the SPI/GPTMS/ESO of 1%, 2.5%, and 5% films. With the addition of ESO was further increased, the surfaces of SPI/GPTMS/ESO of 10% and 15% films became inhomogeneous gradually. Furthermore, compared to the SPI/GPTMS/ESO-2.5% film, the film without GPTMS (the SPI/ESO-2.5% film) contained abundant defects, owing to the poor ESO distribution in SPI matrix, which was consistent with the results of mechanical properties.

Water resistance

The results of moisture content determination, 24-h water absorption, and total soluble matter of the SPI-based films are summarized in Table 5 for comparisons. Since the mainly soluble matter in the films was glycerol and the content remained unchanged to SPI (50%), the total soluble matters of the films ranked 24.3 – 30.0%, without significant difference among them. The moisture content of the SPI film (35.8%) was decreased by 36.2% after adding GPTMS (22.8% SPI/GPTMS film). The moisture content was further reduced by 55.5% after adding 2.5% ESO, compared with the SPI film. The ANOVA test showed a significant reduction at the level of α =

Table 5 Moisture content after condition, water absorption and total soluble matter after 24-h submersion of the SPI-based films.

Film	Moisture content (%)	Water absorption (%)	Total soluble matter (%)
SPI	35.8 (1.2) [a]	209.1 (3.1)	30.0 (0.4)
SPI/GPTMS	22.8 (0.6)	85.2 (10.0)	27.9 (0.7)
SPI/GPTMS/ESO-1%	19.4 (1.1)	78.1 (0.5)	25.2 (0.5)
SPI/GPTMS/ESO-2.5%	15.9 (1.0)	66.8 (1.7)	26.8 (0.6)
SPI/GPTMS/ESO-5%	19.1 (2.4)	45.9 (2.1)	24.7 (1.2)
SPI/GPTMS/ESO-10%	20.4 (0.5)	93.0 (2.2)	26.5 (0.3)
SPI/GPTMS/ESO-15%	19.5 (2.1)	80.5 (0.4)	24.3 (0.6)
SPI/ESO-2.5%	18.7 (0.7)	207.2 (5.0)	28.4 (0.6)

[a] mean (standard deviation).

0.001 (P-value = 5.1×10^{-6}). The results of 24-h water absorption tests (Table 5) showed that the SPI/GPTMS/ESO-5% film had the best water-resistant property (45.9%), which was significantly reduced by 78.1% (ANOVA test, $\alpha = 0.001$, P-value = 5.6×10^{-7}) compared with the SPI film (209.1%). The 24-h water absorption of the SPI/GPTMS/ESO-2.5% film owning the best TE, TS, and YS properties was 66.8%, which was significantly decreased by 68.1% (ANOVA test, $\alpha = 0.001$, P-value = 4.0×10^{-7}) compared with the SPI film. The 24-h water absorption of the SPI/ESO-2.5% film that without GPTMS was 207.2%, which was similar to the SPI film (209.1%). The reason could be the bad distribution of ESO in SPI matrix without the GPTMS effect, resulting in abundant defects (pores) in the film (Fig. 6). The results showed that the water resistance of the SPI film was dramatically improved through the formation of cross-linking network in the modified films.

Conclusions

The tensile modulus, tensile strength, 10% offset yield strength and water resistance of the ESO modified SPI-based films were significantly improved with the presentence of GPTMS. When 2.5% ESO was added, an optimal overall performance of films was achieved. Compared to the unmodified SPI film, TE, TS and YS of the SPI/GPTMS/ESO-2.5% film were increased by 695.6%, 139.8%, and 246.6%, respectively, and the elongation at break was decreased by 67.6%, resulted from the cross-linking reactions between SPI and ESO. Furthermore, the water resistance of the modified films was improved meanwhile. The results of 24-h water absorption tests showed that the SPI/GPTMS/ESO-5% film had the best water-resistant property, which was a 78.1% reduction compared with the unmodified SPI film.

Acknowledgements

This research was supported by the Special Fund for Forestry Research in the Public Interest (Project 201504502), the Beijing Natural Science Foundation (Project 2151003), the National Natural Science Foundation of China (Project 31000268 / C160302), and University of North Texas Research initiation Fund.

Notes and references

1 L. Averous, *J. Macromol. Sci. A,* 2004, **C44**, 231–274.
2 M. Avella, M. E. Errico, R. Rimedio and P. Sadocco, *J. Appl. Polym. Sci.,* 2002, **83**, 1432–1442.
3 J. M. Krochta and C. DeMulderJohnston, *Food Technol-Chicago,* 1997, **51**, 61–74.
4 M. Cruz-Romero and J. Kerry, *CAB Reviews: Perspectives in Agriculture, Veterinary Science, Nutrition and Natural Resources,* 2008, **3**, 25.
5 J. P. Maran, V. Sivakumar, R. Sridhar and V. P. Immanuel, *Ind. Crop. Prod.,* 2013, **42**, 159–168.
6 F. Xu, Y. Dong, W. Zhang, S. Zhang, L. Li and J. Li, *Ind. Crop. Prod.,* 2015, **67**, 373–380.
7 P. Lodha and A. N. Netravali, *Ind. Crop. Prod.,* 2005, **21**, 49–64.
8 J. W. Rhim, A. Gennadios, C. L. Weller and M. A. Hanna, *Ind. Crop. Prod.,* 2002, **15**, 199–205.
9 X. Ren and M. Soucek, in *in Soy-Based Chemicals and Materials,* ed. ed. R. P. Brentin, American Chemical Society, 2014, pp.207-254.
10 P. Tummala, W. Liu, L. T. Drzal, A. K. Mohanty and M. Misra, *Ind. Eng. Chem. Res.,* 2006, **45**, 7491–7496.
11 W. J. Liu, M. Misra, P. Askeland, L. T. Drzal and A. K. Mohanty, *Polymer,* 2005, **46**, 2710–2721.
12 X. Song, C. Zhou, F. Fu, Z. Chen and Q. Wu, *Ind. Crop. Prod.,* 2013, **43**, 538–544.
13 J. A. Foulk and J. M. Bunn, *Ind. Crop. Prod.,* 2001, **14**, 11–22.
14 V. M. Ghorpade and M. A. Hanna, *T. ASAE,* 1996, **39**, 611–615.
15 H. Tian, G. Xu, B. Yang and G. Guo, *J. Food Eng.,* 2011, **107**, 21–26.
16 G. A. Denavi, M. Perez-Mateos, M. C. Anon, P. Montero, A. N. Mauri and M. Carmen Gomez-Guillen, *Food Hydrocolloid.,* 2009, **23**, 2094–2101.
17 S. Y. Ou, Y. Wang, S. Z. Tang, C. H. Huang, M. G. Jackson, *J. Food Eng.,* 2005, **70**, 205–210.
18 D. J. P. Reddy, A. V. Rajulu, V. Arumugam, M. D. Naresh, M. Muthukrishnan, *J. Plast. Film Sheet.,* 2009, **25**, 221-233.
19 L. Chen, G. Remondetto, M. Rouabhia, M. Subirade, *Biomaterials,* 2008, **29**, 3750–3756.
20 A. Gonzalez, M. C. Strumia, C. I. A. Igarzabal, *J. Food Eng.,* 2011, **106**, 331–338.
21 J. W. Rhim, A. Gennadios, C. L. Weller, C. Cezeirat, M. A. Hanna, *Ind. Crop. Prod.,* 1998, 8, 195–203.
22 A. Bigi, G. Cojazzi, S. Panzavolta, K. Rubini and N. Roveri, *Biomaterials,* 2001, **22**, 763–768.
23 C. M. Vaz, P. F. N. M. van Doeveren, G. Yilmaz, L. A. de Graaf, R. L. Reis and A. M. Cunha, *J. Appl. Polym. Sci.,* 2005, **97**, 604–610.
24 C. Marquie, *J. Agric. Food Chem.,* 2001, **49**, 4676–4681.
25 G. Strauss and S. A. Gibson, *Food Hydrocolloid.,* 2004, **18**, 81–89.
26 R. D. Patil, J. E. Mark, A. Apostolov, E. Vassileva and S. Fakirov, *Eur. Polym. J.,* 2000, **36**, 1055–1061.
27 S. J. Park, F. L. Jin and J. R. Lee, *Mat. Sci. Eng. A-Struct.,* 2004, **374**, 109–114.
28 A. M. Díez-Pascual and A. L. Díez-Vicente, *ACS Appl. Mater. Inter.,* 2014, **6**, 17277–17288.
29 I. Mateos-Aparicio, A. R. Cuenca, M. J. Villanueva-Suarez and M. A. Zapata-Revilla, *Nutr. Hosp.,* 2008, **23**, 305–312.
30 Z. Qin, Q. Gao, S. Zhang and J. Li, *Bioresources,* 2013, **8**, 5369–5379.
31 H. Lei, G. Du, Z. Wu, X. Xi and Z. Dong, *Int. J. Adhes. Adhes.,* 2014, **50**, 199–203.
32 K. Luo, S. Zhou, L. Wu and G. Gu, *Langmuir,* 2008, **24**, 11497–11505.
33 C. Li, H. Li, S. Zhang and J. Li, *Bioresources,* 2014, **9**, 5448-5460.
34 Y. Xie, C. A. S. Hill, Z. Xiao, H. Militz and C. Mai, *Composites Part A,* 2010, **41**, 806–819.
35 E. M. Ciannamea, P. M. Stefani and R. A. Ruseckaite, *Food Hydrocolloid.,* 2014, **38**, 193–204.
36 V. Schmidt, C. Giacomelli and V. Soldi, *Polym. Degrad. Stabil.,* 2005, **87**, 25–31.
37 J. Chen, X. Chen, Q. Zhu, F. Chen, X. Zhao and Q. Ao, *J. Sci. Food Agric.,* 2013, **93**, 1687–1691.

Graphical abstract

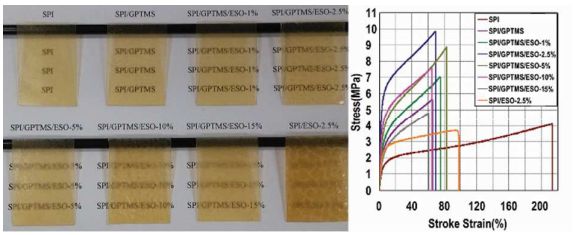

Properties enhancement of soy protein isolate based film by introducing an environmental-friendly cross-linking agent, epoxidized soybean oil.